IOP Conf. Series: Materials Science and Engineering **932** (2020) 012052 doi:10.1088/1757-899X/932/1/012052

Strain monitoring for shallow foundation using the application of Brillouin Optical Time Domain Analysis sensing system (BOTDA)

Qurratu Aini Sirat[1*], Dayangku Salma Awang Ismail[2], Izwan Shah Ahmad[1], Azman Kassim[3]

[1]Postgraduate, School of Civil Engineering, Universiti Teknologi Malaysia, 81310 Johor Bahru, Johor, Malaysia

[2]Lecturer, Faculty of Civil Engineering, Universiti Malaysia Sarawak, 943000 Kota Samarahan, Sarawak, Malaysia

[3]Prof Lecturer, School of Civil Engineering, Universiti Teknologi Malaysia, 81310 Johor Bahru, Johor, Malaysia

*E-mail: qurratu@civil.my

Abstract. Stability analysis of the foundation is closely associated with soil deformations and since the stability of the foundation affect the stability of the entire structure, instrumentation and monitoring play an important role in monitoring its performances. The usage of Brillouin Optical Time Domain Analysis (BOTDA) sensing system is implemented in this study to monitor the soil deformation, yet the accuracy of the fiber sensing technology is still a concerned point. Thus, the aims of the paper are to evaluate the parameter configuration of the BOTDA interrogator and to analyze the fiber optic-soil interaction from the strain distribution data under the influence of incremental surcharge loading. The methodology presented are experimental works for calibration of fiber optic as for acquiring the coefficients by calibrating the signal difference in terms of strain and thermal characteristics. Then, the coefficients use used in a small-scale physical model to observe the fiber optic-soil interaction under the influence of surcharge loading. From the result of this study, the coefficient over a Brillouin signal for Fujikura optical fiber is 20 με and 1°C for strain and temperature respectively. The fiber-soil interface also increases with the implementation of anchorage system. In conclusion, optical fiber sensing is a good approach for instrumentations and monitoring for geotechnical structures as fiber optics is sensitive to the movement of the soil.

1. Introduction

The burden exerted on the surface of the ground through foundation caused various ground displacement or deformation in shallow foundation situation. This deformation is better determined by soil settling measurements. The burden imposed on the soil can be attributed to the soil weight and/or added burden while loaded, which is often known as surcharge loading. The research of stress transfer

to the soil is necessary to understand the mechanism in the settlement of foundation. Instrumentation and monitoring therefore play an important role in the analysis of soil behavior and soil stability. Over the last decade, the performance of geotechnical structures was commonly examined using common conventional practices. Nevertheless, common instrumentation such as inclinometers, the Global Positioning System (GPS) and soil deformation measuring methods have certain drawbacks in terms of their measuring distance or accuracy [1]. As natural consequences, optical fiber sensing technology has been used in geotechnical engineering as a monitoring method, as optical fiber systems are cheap, can thrive under harsh conditions and measurements can be carried out along fiber optics for thousands of kilometers [2,3].

For the past few decades, there are many studies to evaluate the soil deformations by using the application of optical fiber sensing by embedding it directly within soil mass [4,5,6,7]. The precision of fiber sensing technologies is also a challenge because the precision relies on the fiber optic configuration and the contact between the optic fiber and the soil. To get the exact value of strain and temperature, the parameter configuration input must be entered correctly as different fiber optic types have different strain and temperature coefficient values. Therefore, the efficacy of the fiber optic in calculating the strain relies on interaction between the fiber optic and soil where a proper contact will result the correct amount of strain [2]. In addition, the poor-quality on the deployment of the sensors and temperature adjustment are the risk element of the inconsistencies in fiber optic measurements [8]. Thus, this paper introduces the laboratory technique beginning with the calibration phase of Fujikura optical fiber accompanied by a small-scale physical simulation test. The implementation of the anchorage method in the analysis of the stability of the shallow foundation due to exerted loading will help to improve the efficiency of the soil-structure interaction.

So far as the practical approach is concerned, laboratory experiments in small-scale physical simulation which reflect the specific conditions of the geotechnical structures are also used as a means of stimulating soil behaviour because the research of a full-scale base framework is expensive , time-consuming and impractical to conduct [9]. In order to analyze the problems of geotechnical engineering, the small-scale physical model is chosen for its advantages of sized reductions, simplification and simplicity, possible study of too complicated analytical structures and possible use of laboratory data as well as testing by theoretical and computational methods [10].

2. Materials and method

2.1 Calibration of Fiber Optic

The 12-ribbon Fujikura is used for this analysis as the cable for strain sensing and the cross section of the fiber shown in Figure 1. The cable comprises of 12 fibers with protected coatings in varying colours. The dimension of 12 ribbon fiber is 3 mm in width and roughly 0.3 mm in thickness. The optical fiber is ideal for being the sensing cable for direct embedding in the soil layer, owing to the wider surface or area of contact. The primary objective of the test is to determine the relationship between Brillouin 's shift frequency and obtained strain value then to correctly enter the value of the strain and temperature coefficients at BOTDA Analyzer because various fiber optic forms have different strain and temperature coefficient values.

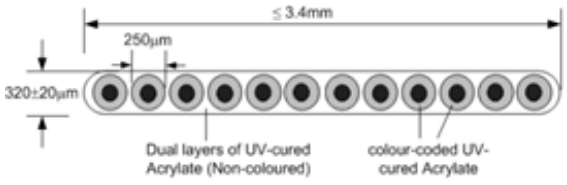

Figure 1. Cross section of 12-ribbon Fujikura [5].

2.1.1 Calibration method for the coefficient of strain. As seen in Figure 2, the fiber optic was configured using a developed strain rig set-up with a ball-bearing guiding pad on the left side. The other end is a fixed clamp and the set-up attached to the load cell with shape 'S 'as seen in Figure 3 and can be mounted on the latter end side of the set-up of the strain rig. A 20 m of fiber length was planned for the calibration analysis and the strained segment at 8 m and 9 m locations was defined to be the length of the sample. Initially, the baseline reading is set and proceeded by pulling per 1 mm and the BOTDA interrogator will acquired the calculated strain.

Figure 2. Fabricated tensile test for fiber optic.

Figure 3. Load cell to obtain tensile force data.

2.1.2 Calibration method for the coefficient of temperature. The fiber optic was tested to an 8.1 cm length, 5.1 cm width and 2.8 cm height Memmert water bath tank where the setup set-up is seen in Figure 4. A total of 20 m of fiber length and roughly 5 m of fiber length is inserted in the water bath, which was between 8 m and 12 m of overall length. The temperature was used as a reference read at 23 degrees Celsius (tap water). The temperature value was set with a 10-degree increment and increasing temperature reading of the strain data was recorded; beginning from 31, 41, 52, 61 and 72 degrees Celsius.

Figure 4. Memmert Water Bath.

2.2 Experimental Works (Physical Modeling).
A small 1 G model portraying the real structure, with measurements 1.0 m (Length), 0.3 m (Width) and 0.8 m (Height), was prepared and designed. Within the premises of Universiti Teknologi Malaysia (UTM), Johor Bahru campus, the soil used for this research was acquired. The soil was compacted into four (4) layers and the fiber optic was placed in between the soil layers for the lower, middle and top layers strain responses. The fiber optic is horizontally mounted and is opposite to the surcharge loading. During the testing period, a small scale 1 G model of a shallow foundation described by a

load plate test under gradual overloading was stimulated to assess soil stability. Plate measure with a width of 300 mm and a length of 150 mm. The BOTDA analyzer, also known as the Distributed Strain and Temperature Sensor (DSTS), attached the optical connectors. Measurements of fiber optic were rendered using DSTS when exerting pressure on the load of the plate. The outcome was the response of the strain distribution assessed by the fiber optic imbedded in the soil.

3. Results and discussion

3.1 Strain Coefficient (C_ε)

Only up to 10 mm elongation was performed in the calibration experiment, and the strained section was from 7.7 m to 8.7 m (middle length of fiber). As for measurement data obtained, the attention needs to be given to the middle part of the frequency distribution (see Figure 6) for accurate frequency reading. The constant frequency distribution was then summed over 10 points and graph is plotted as seen in Figure 7. The graph represented the association between the tensile force applied and the degree of changes in frequency which it contributed to the coefficient of strain. Therefore, the 1 MHz of the frequency signal is equivalent to 20 micro strain ($\mu\varepsilon$).

3.2 Temperature Coefficient (C_T)

A baseline reading was assigned for the temperature coefficient at a temperature of 23°C. For temperature coefficient, the submerged section was from 8.0 m to 12.0 m. The method of tabulating the graph will be the same as strain coefficient where attention will be given to the middle part of the frequency distribution. The average frequency value (vb) was determined by taking the average constant frequency reading describing a submerged portion of the optical fiber (see just 2 m of submerged duration as seen in Figure 8). Figure 9 demonstrates the constant temperature differential interaction against Brillouin frequency change, Δvb. The temperature coefficient obtained is 0.9977, roughly 1 C / MHz.

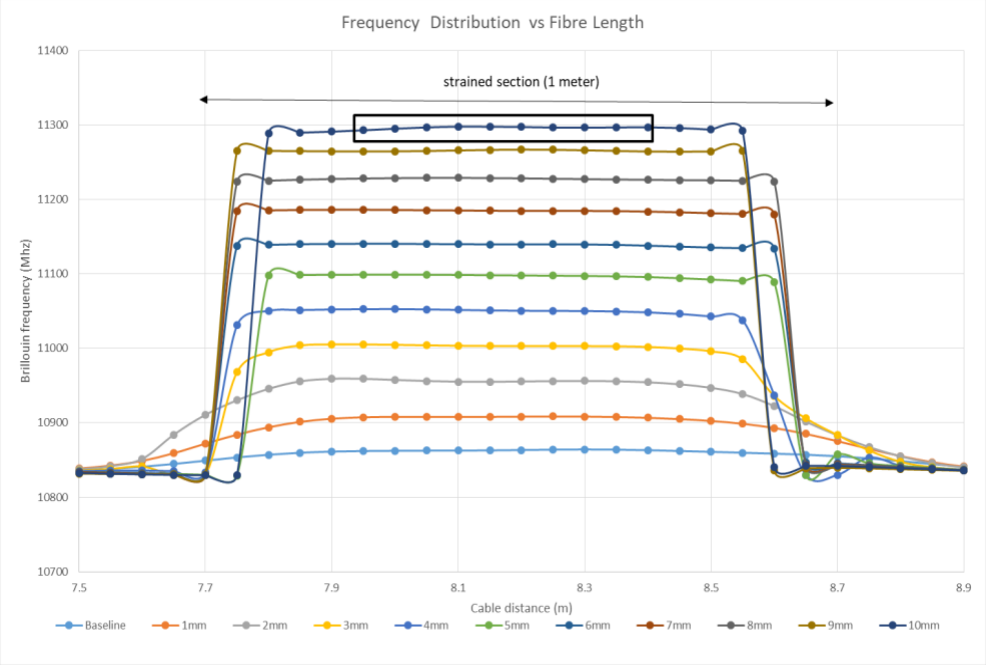

Figure 6. Averaging of frequency for the relationship of frequency against strain.

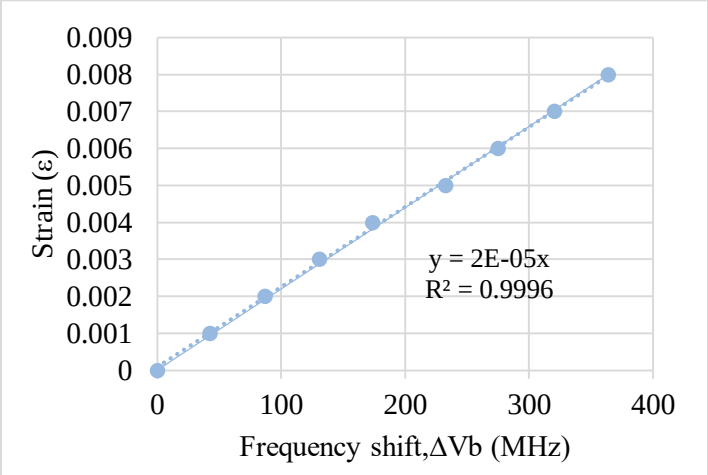

Figure 7. The graph of strain coefficient (C_ε).

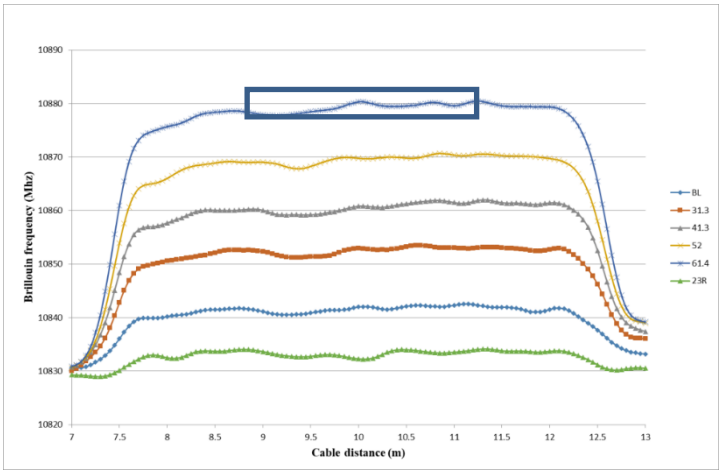

Figure 8. Averaging of frequency for the relationship of frequency against temperature.

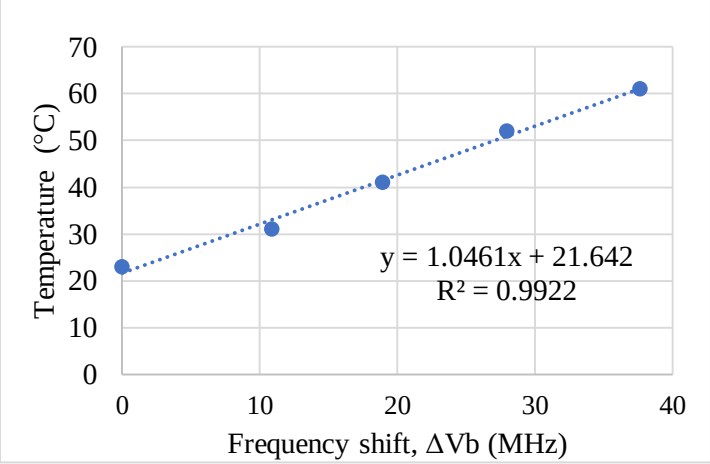

Figure 9. The graph of strain coefficient (C_T).

3.3 Strain Distribution due to Surcharge Loading

Throughout the plate load experiment, the surcharge load applied was 1 kN, 3 kN, 5 kN, 7 kN, 9 kN, 12 kN, 13 kN, 14 kN and 15 kN. The research was carried out in phase loading where the pressure stopped as the data were taken at each of the loads specified. At each load, the frequency was measured. The surcharge loading was stopped at 15kN because the frequency distribution in the BODTA Analyzer shows odd trend as the soil begins to fail at 15kN load. Just before the study, baseline reading was taken where the initial Brillouin frequency distribution would be used as a reference for other readings. Therefore, the calculated data were correlated with the baseline and the discrepancy between the two data frequencies was translated into strain by multiplying the findings with the strain coefficient obtained previously [20 με/MHz].

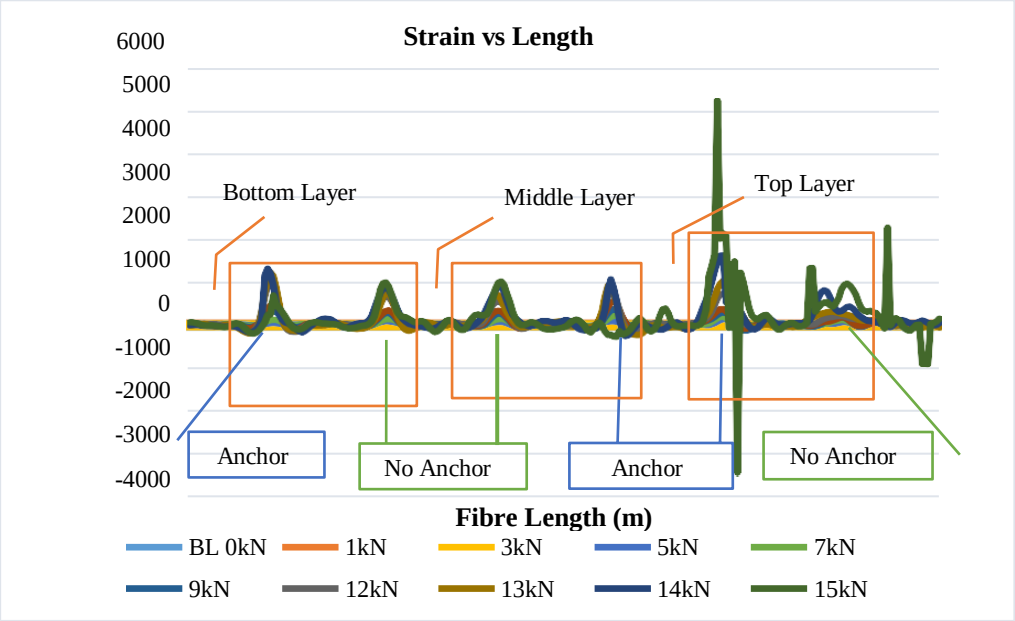

Figure 10. Strain vs Fiber length.

For each load, a graph for strain distribution was tabulated against optical fiber length as shown in Figure 10. The overall fiber optic range was 21 m. It illustrates that from Figure 10 that 15kN surcharge load has given higher strain distribution compared with the rest of the load. The greater the surcharge load mounted to the soil mass, the greater the stress values because the higher loads mean higher stresses working on the soil resulting in higher deformations within the soil mass and resulting in higher strain values. Figure 10 also displays the strain graph for the lower, center, and top layers of soil while performing the load test. Every soil layer consists of two graphs where one graph represents anchor fiber, while the other represents anchor-free fiber optic. The location of the fiber optic for both anchors and no anchors has been alternated from the bottom layer to the topsoil layer owing to the fiber deployment strategies inside the chamber and the relation of the strain measurements between them will be addressed in the next sub-chapter.

3.4 Interaction between Fiber optic and Soil

Figure 11, Figure 12 and Figure 13 display the effects of an anchor fiber optic and non-anchor fiber for the top, middle and bottom layers respectively. In this study, two fiber optic approaches have been applied to evaluate the relationship between fiber optic and soil.

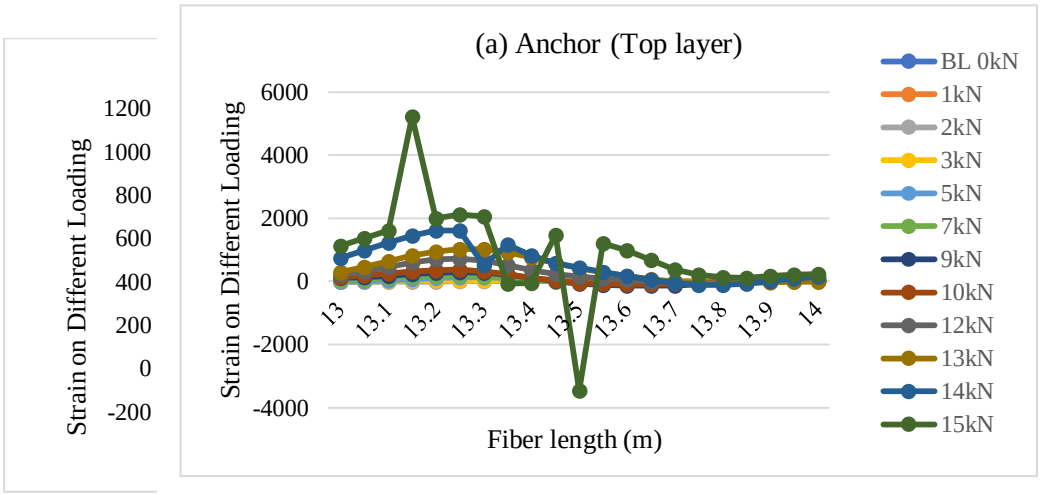

Figure 11. Top layer (a) anchor and (b) non-anchor fiber optic strain distribution.

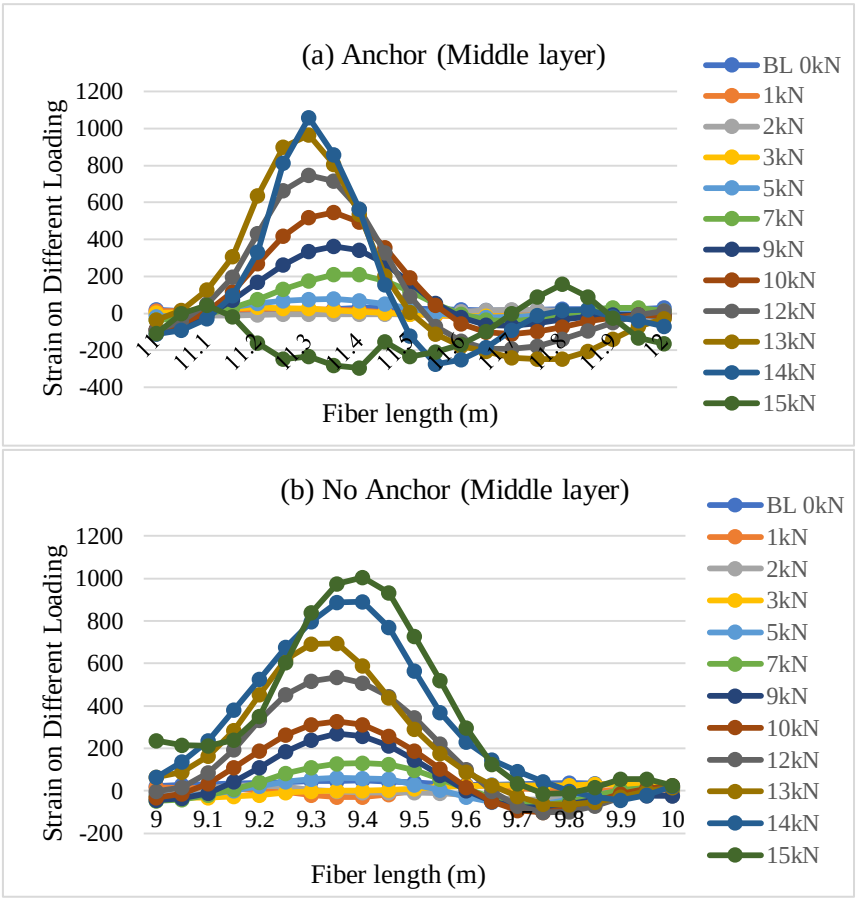

Figure 12. Middle layer (a) anchor and (b) non-anchor fiber optic strain distribution.

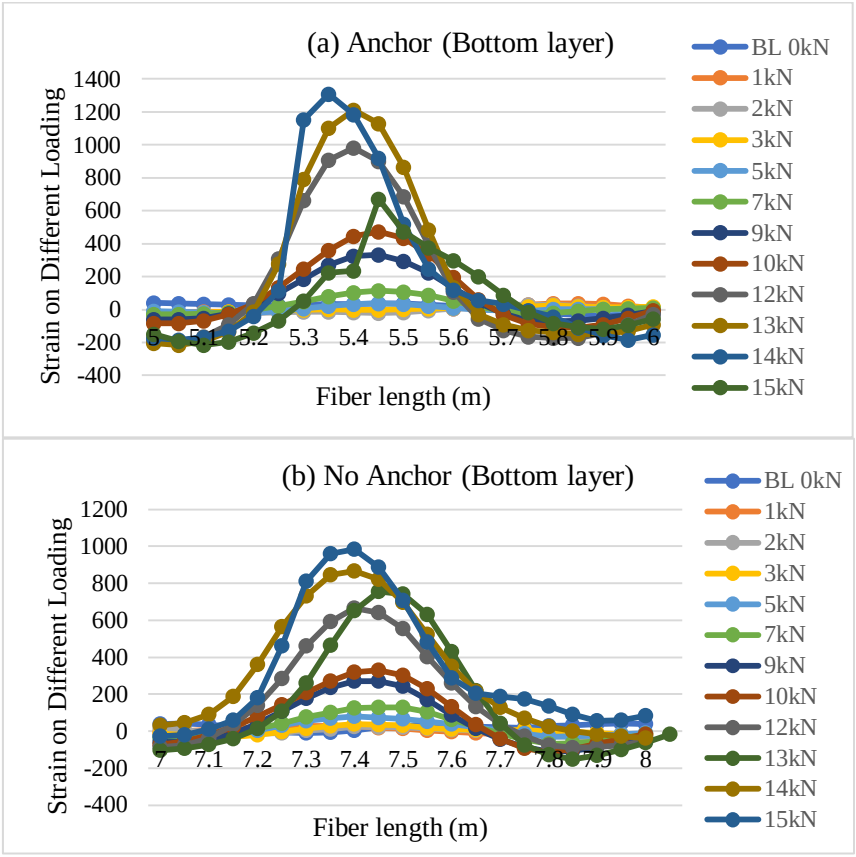

Figure 13. Bottom layer (a) anchor and (b) non-anchor fiber optic strain distribution.

From an overall standpoint, all experimental tests for anchor and non-anchor connection approaches indicate that fiber optics are prone to nearby ground changes where it can scale up to micro strains (μb). In addition, the anchorage method provides better outcomes since the strain values are marginally higher than non-anchor fiber optic values. Thus, anchor fiber optic is more reactive and effective because it has higher strain values resulting in improved contact with optical fiber and soil.

Conclusion

As far as the conclusion is concerned, profound understanding in the characteristics of the BOTDA device and the optical fiber sensor before any test is start is important to minimize the errors during experimental works and analyzing the slope structure. The findings of the plotted graph demonstrate that the strain and temperature coefficient for the optical fiber of 12 ribbon Fujikura is 20 με and 1°C over a Megahertz of Brillouin signal, respectively. The plotted graph has resulted in improved strain distribution of the anchorage where measurement up to micro strain (με) can be taken. Furthermore, fiber optics are extremely sensitive to slight soil movement, cheap and capable of measuring strain through the fiber rather than isolated points which makes it suitable as the geotechnical sensors.

References

[1] Lienhart, W, 2015. Case studies of high-sensitivity monitoring of natural and engineered slopes. J. Rock Mech. Geotech. Eng. 7, 379–384.
[2] Dong, Y., Chen, L. & Bao, X., 2011. Time-division multiplexing-based BOTDA over 100 km sensing length. Opt. Lett. 36, 277–279.
[3] C. C. Zhang, H. H. Zhu, and B. Shi, 2016. Role of the interface between distributed fibre optic

strain sensor and soil in ground deformation measurement, Sci. Rep., vol. **6**, no. October, pp. 1–9.

[4] Wang, B. J., Li, K., Shi, B. & Wei, G. Q., 2009. Test on application of distributed fiber optic sensing technique into soil slope monitoring. Landslides 6, 61–68.

[5] Zhu, H. H., Shi, B., Zhang, J., Yan, J. F. & Zhang, C. C., 2014. Distributed fiber optic monitoring and stability analysis of a model slope under surcharge loading. J. Mt. Sci. 11, 979–989.

[6] Zeni, L. et al., 2015. Brillouin optical time-domain analysis for geotechnical monitoring. J. Rock Mech. Geotech. Eng. 7, 458–462.

[7] Picarelli, L. et al., 2015. Performance of slope behavior indicators in unsaturated pyroclastic soils. J. Mt. Sci. 12, 1434–1447.

[8] H. Mohamad, 2008. Distributed Optical Fibre Strain Sensing of Geotechnical Structures, Ph.D. dissertation, Dept. of Eng., University of Cambridge.

[9] A. Altaee and B. H. Fellenius 2011. Physical modeling in sand. Canadian Geotechnical Journal. **31**. 420-431. 10.1139/t94-049.

[10] M. Al Heib, F. HdrEmeriault, M. Caudron, L. Nghiem, and B. Hor, 2013. Large-scale soil–structure physical model (1 g) – assessment of structure damages, *Int. J. Phys. Model. Geotech.*, vol. **13**, no. 4, pp. 138–152.

Acknowledgements
The author gratefully acknowledges the support of the Universiti Teknologi Malaysia (UTM) and the Ministry of Higher Education through the awarded Research University Grant (GUP), vote number Q.J130000.2522.19H77 is highly appreciated.